High resolution spectroscopy of the post-red supergiant IRC+10420

Oudmaijer, R. D.

Published in:
Astronomy & astrophysics supplement series

DOI:
10.1051/aas:1998404

Publication date:
1998

ASTRONOMY & ASTROPHYSICS
SUPPLEMENT SERIES

Astron. Astrophys. Suppl. Ser. **129,** 541-552 (1998)

High resolution spectroscopy of the post-red supergiant IRC+10420

I. The data⋆

R.D. Oudmaijer

[1] Imperial College of Science, Technology and Medicine, Blackett Laboratory, Prince Consort Road, London, SW7 2BZ, UK
[2] Kapteyn Astronomical Institute, P.O. Box 800, NL-9700 AV Groningen, The Netherlands

Received September 5; accepted October 27, 1997

Abstract. A high resolution optical spectrum of the post-red supergiant candidate IRC+10420 is presented. The Utrecht Echelle Spectrograph observations, with a total integration time of more than 9 hours, provide a spectral coverage from 3850 Å to 1 μm, and a spectral resolution of 9 km s^{-1}. The spectrum is shown, and an identification list of lines in the spectrum is provided. From a preliminary analysis of the spectrum we find that the spectral type of IRC+10420 has changed from F8I$^+$ in 1973 to mid- to early A type now, confirming the results of Oudmaijer et al. (1996), who claimed a change in temperature based on photometric changes. It is shown that most of the emission lines in the spectrum of IRC+10420 are blue-shifted with respect to the systemic velocity traced by circumstellar rotational CO emission, while the (few) absorption lines - with the exception of some high excitation lines - are red-shifted by 25 km s^{-1}, which may suggest infall of material onto the star. Finally, it is found that the interstellar extinction towards IRC+10420 as traced by the Diffuse Interstellar Bands is very large, with an inferred *E(B–V)* of 1.4 ± 0.5 compared to a total *E(B–V)* of 2.4.

Key words: stars: circumstellar matter — stars: emission-line, Be — stars: individual: IRC+10420 — stars: AGB and post-AGB — stars: supergiants

1. Introduction

The hypergiant IRC+10420 (19h24m26.7s +11d15m10.9s, (1950.0)) is an enigmatic star. At present it is believed that IRC+10420 is a massive star evolving from the Red Supergiant Branch (RSG) to the Wolf-Rayet phase. (Jones et al. 1993; Humphreys 1991; Nedoluha & Bowers 1992; Oudmaijer et al. 1996, hereafter Paper I). Whereas the sample of massive evolved stars is relatively large, the number of transition objects between the RSG phase and hotter objects is comparatively small. Recently, Kastner & Weintraub (1995) proposed the G-type supergiant HD 179821 to be a post-Red Supergiant objects as well, but a subsequent abundance analysis by Začs et al. (1996) indicates, based on the overabundance of *s*-processed elements, that it is in fact a low mass evolved object. So far, IRC+10420 is the only object known in this transition phase.

The optical and near-infrared spectra of IRC+10420 appear to be variable. Humphreys et al. (1973) obtained the first optical spectrum of IRC+10420, and did not mention the presence of emission lines. Another optical spectrum covering Hα was obtained by Fix (1981), who did not mention emission either. Hα emission was first reported by Irvine (1986), along with the detection of [CaII] and [FeII] lines. Oudmaijer et al. (1994) discovered emission in near-infrared hydrogen recombination lines of IRC+10420. Based on changes in the spectral energy distribution, it is suggested in Paper I that the spectral type of IRC+10420 has changed from F8I$^+$ to considerably higher temperatures, implying that IRC+10420 is on an evolutionary track towards the left in the HR diagram.

In light of the long term changes of the spectrum and spectral type of IRC+10420, the faintness of IRC+10420 in the blue, as well as its highly peculiar spectrum, we present the high resolution spectrum that we have obtained in July 1994 for future reference. The spectra were taken with the Utrecht Echelle Spectrograph mounted on the 4.2 m William Herschel Telescope. The resulting spectrum covers 3850 Å−1 μm.

This paper is organized as follows: In Sect. 2, we present the observations and data reduction, Sect. 3

Send offprint requests to: R.D. Oudmaijer
e-mail: r.oudmaijer@ic.ac.uk

⋆ Table B1 is only available at the CDS via anonymous ftp 130.79.128.5 or at http://cdsweb.u-strasbg.fr/Abstract.html

discusses briefly the spectral type, line profiles and the interstellar reddening traced by Diffuse Interstellar Bands. We conclude in Sect. 4 with some final remarks, while the Appendix contains the spectrum, the table of line identifications is available electronically at CDS.

2. Observations and data-reduction

2.1. The Utrecht Echelle Spectrograph

We employed the Utrecht Echelle Spectrograph (UES, Unger 1994), mounted on the Nasmyth platform of the 4.2 m William Herschel Telescope, La Palma, Spain. The UES achieves a spectral resolution of $\lambda/\Delta\lambda \sim 30\,000$. Large prisms are used for the cross-dispersion instead of a grating, which makes the throughput of the system ($\sim 80\%$) larger than usual. The main aim of the observations of IRC+10420 was to obtain velocity resolved spectra of the entire optical spectrum at high signal-to-noise.

The observations were carried out during the nights of July 26/27 and 27/28 1994. The UES 31 grooves/mm setting which provides a large wavelength coverage was used. Due to strong western winds the atmospheric (grey) extinction was very high, which, especially in the blue spectra, led to lower signal-to-noise (SNR) spectra than expected. However, due to probably the same dust, the atmosphere was extremely stable, resulting in measured seeing less than $1''$. The slit width during these observations was $1''$. In the second part of the last night the grey extinction was virtually gone, but this was paid for with a seeing of order $3''$, and a slit with a width of $2.5''$ was inserted. The larger slit effectively degraded the spectral resolution by a factor 2. IRC+10420 was measured in 4 wavelength settings. Observations of the blue part of the spectrum were performed with a central wavelength of 4253 Å. In this set-up the spectrum was covered from 3832 to 4936 Å in 33 orders. The "green" part of the spectrum was observed with $\lambda_{\rm central} = 5261$ Å ($4482 - 6714$ Å in 42 orders). For the red part, two different settings were used, since at longer wavelengths the CCD is too small to cover the entire wavelength range. These settings were performed with $\lambda_{\rm central} = 7110$ Å (covering $5551 - 10\,0201$ Å in 47 orders) and $\lambda_{\rm central} = 7156$ Å ($5588 - 10\,0452$ Å in 48 orders). The detector was a 1024×1024 TEK CCD.

IRC+10420 has a very red spectral energy distribution with $R \sim 9$, $B \sim 14$ (see e.g. Paper I). Exposure times of 20 min resulted in high signal-to-noise (SNR) spectra in the red, whereas a total of 6h45m was spent in the blue part where the SNR ranged from ≈ 12 at 3900 Å to ≈ 100 at 4900 Å. In order to prevent the number of cosmic ray events from reaching unacceptably high values, the maximum integration times were limited to 30 min. By paying the price of a slightly lower SNR, these cosmic ray events were removed during the reduction procedure by median filtering the individual spectra.

In addition to IRC+10420, hot stars with few lines in their spectra were observed to divide out telluric absorption features. This was done for the red settings ($\lambda_{\rm central} = 7110$ and 7156 Å), using HR 7318 (B0.5 IV) and HR 6175 (O9V) respectively. These spectra were continuum normalized using high order polynomials to remove the broad stellar absorption lines. The strength of the telluric absorption features were then matched in equivalent width with those observed in the spectrum of IRC+10420. The division works very well to remove the telluric absorption lines in most instances, but in the wavelength regimes where the telluric lines are saturated, residuals inevitably remain in the spectrum.

Wavelength calibration was performed by observing a Thorium-Argon lamp after each stellar exposure if the telescope had moved to another position. Otherwise, the lamp was observed hourly. Flatfields were obtained by observing the spectrum of a Tungsten lamp. The velocity resolution measured from the full-width-at-half-maximum (FWHM) was $8-9$ km s^{-1}. A log of the observations is provided in Table 1.

Table 1. Log of the UES observations

Object	$\lambda_{\rm central}$ (Å)	Integration time (s)	date
IRC+10420	5261	2×900	26/07/94
IRC+10420	5261	1800	27/07/94
IRC+10420	4253	5×1800	27/07/94
IRC+10420	7110	1200	27/07/94
IRC+10420	7156	2×1800	27/07/94
IRC+10420	4253	8×1800, 1×900	28/07/94

2.2. Data reduction

The data were reduced with the echelle reduction package available in IRAF[1]. The data were bias-subtracted first by fitting the overscan regions of the CCD. As there is a light leak towards the overscan regions, the bright flatfields showed a slight excess above the nominal bias values. The leakage only has a small effect on the resulting flatfields since its magnitude is low with respect to the counts resulting from the flatfields. It is hardly detectable in the stellar spectra.

Flatfields were constructed by median filtering and coadding all flatfields. In the case of the TEK detector, flatfielding is critically needed for the longer wavelength region where dramatic fringing occurs. Most of the fringing

[1] IRAF (Tody 1993) is distributed by the National Optical Astronomy Observatories, which is operated by the Association of Universities for Research in Astronomy, Inc. under cooperative agreement with the National Science Foundation.

in the stellar spectra can be removed by dividing by the flatfield. After tracing the different orders of the frames of a bright source, the flatfields were normalized, and the stellar images flatfielded. The individual orders were then optimally extracted with a variance weighting algorithm. For the brighter spectra it was possible to effectively reject those pixels affected by cosmic ray events during the extraction. For the lower SNR spectra in the blue, the cosmic ray rejection did not work properly, and the cosmic rays were removed by median filtering the exposures. The sky emission in the blue spectra was subtracted by extracting several rows adjacent to the stellar spectra, and applying a continuum fit to the sky-spectrum. The fit was then subtracted from the original signal. Wavelength calibration was performed by fitting respectively $4^{\rm th}$ and $5^{\rm th}$ order polynomials in the dispersion and cross dispersion directions to the lines of the Th-Ar lamp spectra. The fits through the more than $400-500$ identified lines had 1σ errors of less than one tenth of a pixel. Tests indicate that a shift in wavelength during the observations amounted to half a pixel (≈ 4 km s^{-1}). The individual orders were rectified and merged into one spectrum to exploit the fact that the SNR increased in cases where the orders overlapped in wavelength.

2.3. Hα spectroscopy

Since the Hα line wings extend to large velocities, the individual orders of the echelle spectrograph are too small to cover the entire line. Therefore, IRC+10420 was observed in service time on 6 September 1993 with the Intermediate Dispersion Spectrograph mounted on the 2.5 m Isaac Newton Telescope, La Palma, Spain. The H2400B grating centered on Hα with a 1180 × 1180 EEV5 CCD chip were employed. This grating provides a resolution of 15 km s^{-1}, and a wavelength coverage of $6475-6650$ Å. Wavelength calibration was done using a Copper-Neon lamp. IRC+10420 was observed 3 × 512 s. The data were reduced in the standard way.

2.4. Line identification

The optical spectrum of IRC+10420 is characterized by a large number of absorption lines, emission lines, and absorption lines that are partly filled in with emission. Due to the rather non-standard spectrum, it was decided to identify the lines manually using the multiplet table of Moore (1945). Starting with the strongest lines, it was possible to identify the stronger lines in the spectrum by comparing the measured strength and velocity of the lines with the intrinsic strength given in Moore (1945). Many unidentified absorption lines could be attributed to the "Diffuse Interstellar Bands" in the catalog of Jenniskens & Désert (1994, hereafter JD94).

The resulting spectrum of IRC+10420 is presented in Fig. 5, while several strong hydrogen lines and calcium lines are presented separately in Figs. 3 and 4. The identified lines and their data are provided in Table B1.

3. The spectrum of IRC+10420

In this section we briefly touch upon the global characteristics of the spectrum. The spectrum is dominated by absorption and emission lines of neutral and singly ionized Fe, TiII, CrII as well as NI, OI, SiII, and the high order hydrogen recombination lines of the Balmer and Paschen series. We also identify a weak line at λ5875 with HeI. All lines are broad, especially the asymmetric and red-shifted absorption lines have FWHM values of order 1 Å.

3.1. The spectral type

In 1973, Humphreys et al. (1973) determined the spectral type of IRC+10420 as F8Ia$^+$. The late spectral type was based on the presence of the G-band in the spectrum, the high luminosity was based on the strong OI triplet at 7774 Å. The present spectrum of IRC+10420 does not agree with an F8 classification; the lack of neutral lines and the presence of a helium line certainly suggest an earlier spectral type. In Paper I we investigated the spectral energy distribution of IRC+10420 , and found changes in the photometry over the last 20 years. During this epoch the V band magnitude remained essentially constant, while the *(V – J)* and *(V – K)* colours changed by 0.75 magnitudes. These colour changes were explained as the result of an increase of the photospheric temperature of about 1000 K. The presence of HeI absorption confirms that the spectral type is earlier than F8. A new determination of the spectral type is thus warranted. This poses a problem in the case of IRC+10420 . Normal classification criteria use line ratios that are based on lower resolution spectra, where the effects of blended lines are taken into account. In the case of IRC+10420 , the emission lines do not provide the best basis for such a procedure. In addition, the large number of emission lines makes comparison with lower resolution standard spectra very difficult. New spectral classification criteria and/or a new catalog of spectral standard stars based on higher resolution spectra would be desirable.

In the course of our study of IRC+10420 and other studies with the UES we have collected some spectra of standard stars which we will use here to make a crude estimate of the spectral type of IRC+10420 . During the observations of IRC+10420 for this paper we observed HR 7796 (F8I) and α Cyg (A2I) as comparison. The F supergiants HR 1017 (F5I) and HR 1865 (F0I) were observed for another study (Oudmaijer & Bakker 1994). The overlapping part of the spectra of these four objects was limited to the wavelength range $4690-4935$ Å. The spectra of these 4 stars and that of IRC+10420 are plotted in Fig. 1. Despite the small wavelength coverage, the differences between the spectra are significant; The F type

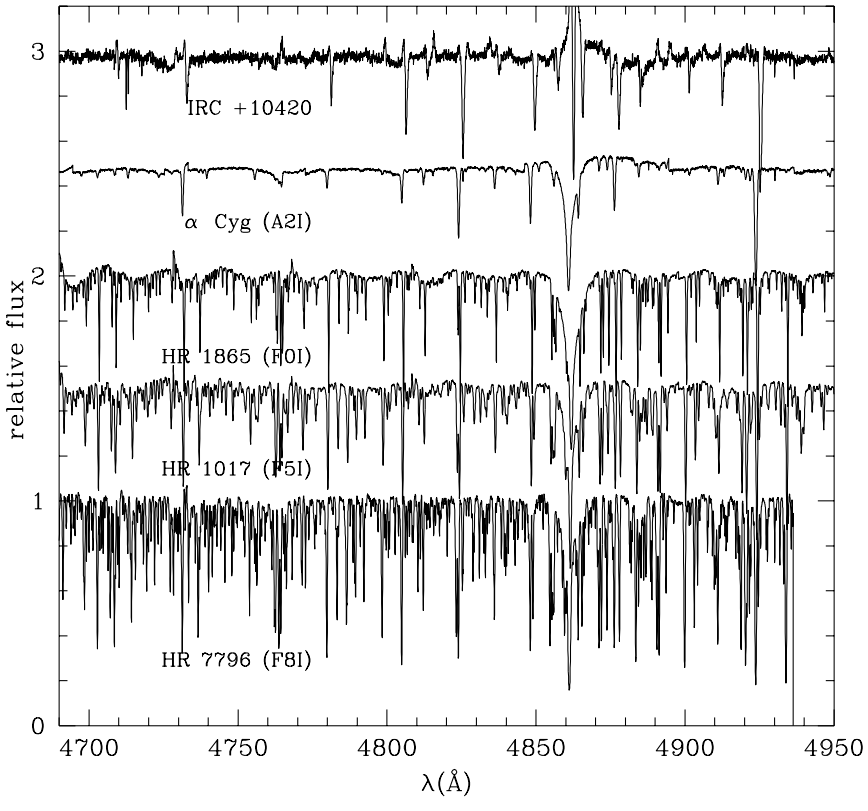

Fig. 1. UES spectra of IRC+10420 and four spectral standard stars in the wavelength range 4690 − 4935 Å. Note that the continua of the F supergiants seem to fluctuate. This is the consequence of difficulties in normalizing the spectra due to the large number of lines

stars show a large number of (neutral) absorption lines. The neutral lines decrease in strength going from F8 to F0, and are not present in the spectrum of the A2I star, where Hβ and singly ionized metal lines are present.

IRC+10420 best resembles the A2I spectrum, based on the lack of neutral lines, and is intermediate between F0 and A2 as evident from the strength of the strong absorption lines due to Fe and Cr in the spectra. IRC+10420 definitely does not resemble an F8 star. From the comparison of the spectra we conclude that the spectrum of IRC+10420 is intermediate between F0 and A2, and possibly even earlier than A5. This implies that the spectrum of IRC+10420 has changed from F8 in 1973 (Humphreys et al. 1973) to A type in 1994. Such a change in spectral type is consistent with the change in the continuum energy distribution (Paper I). During the final stages of the preparation of this paper, some of these data were used for an abundance study by Klochkova et al. (1997), which also points to an increase in temperature, while the abundances appear to be consistent with a massive evolutionary phase of the object.

3.2. Line velocities

Apart from the line profiles, the central velocities of the lines show a marked behaviour, which we will briefly touch upon here. The systemic velocity of the system is 75 km s^{-1} as found in the CO rotational lines in Paper I, which is also measured for the high excitation HeI λ5875 and some high excitation SiII lines. Surprisingly, there is a large variation in central velocities of the different types of line. Except for the above mentioned lines, virtually all absorption lines, including other high excitation lines due to C, N, and O, are *red*-shifted by a considerable amount with respect to the systemic velocity. We also note that the central velocities of forbidden lines as e.g. presented in Fig. 4, are red-shifted (by 10 − 20 km s^{-1}) from the systemic velocity.

In Fig. 2 we show the relation between the observed peak velocity of the emission and absorption lines of FeII as function of oscillator strength. The absorption lines have a constant velocity of 104 ± 5 km s^{-1} over the entire range of oscillator strength. This holds for multiplets with only absorption lines and multiplets that have both

emission and absorption lines. The emission lines however show a different picture. As the absorption strength decreases, the peak velocities of the lines shift towards the systemic velocity. This observed correlation between the emission peak-velocities with the oscillator strength also holds for the other metals as Cr, Ti and Sc, for which the velocity of the absorption lines is constant with absorption strength at $\sim$ 100 km s^{-1}. This is not what one would expect if the lineprofiles are the result of a superposition of an emission component centered around the systemic velocity and an underlying red-shifted photospheric absorption component. In that case, one would expect that the velocity of the peak of the emission would shift towards the systemic velocity for a decreasing absorption strength. This is observed, but one would also expect the absorption minimum to shift towards larger red-shifts, which is not observed. Instead, there appears a constant absorption component at +25 km s^{-1} with respect to the stellar velocity. Indeed, if (red-shifted) absorption is superposed on an underlying emission, one can expect the emission line velocities to change, while the absorption line centers remain at the same velocity.

As a side-result, the lower panel in Fig. 2 shows the peak velocities as function of wavelength. There is no correlation between the two. This result contradicts the model of Fix (1981) that the red-shift of the photosphere was the result of multiple scattering of photons by circumstellar dust. In this model it is predicted that the line in the blue part of the spectrum are considerably more red-shifted than those at longer wavelengths, which is not seen in our data.

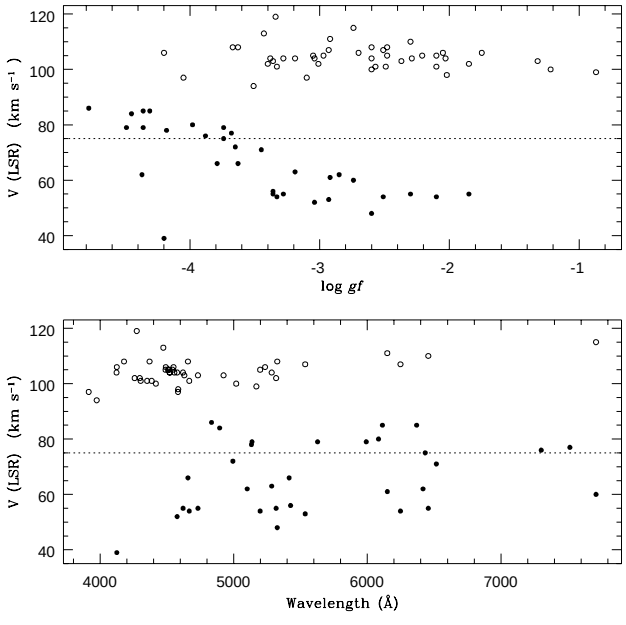

Fig. 2. Relation between the observed central velocities of the FeII lines and the oscillator strengths (upper panel) and wavelength (lower panel). The open dots denote the absorption lines, the filled dots represent the emission lines

3.3. Interstellar extinction and the Diffuse Interstellar Bands

IRC+10420 is a very reddened object, In Paper I we used Kurucz models to fit the spectral energy distribution of IRC+10420 and found a total *E(B–V)* towards IRC+10420 of $\sim$ 2.4. Of course, it is hard to disentangle the combined effects of circumstellar and interstellar extinction towards this objects, but the presence of many strong Diffuse Interstellar Bands (DIBs) in the absorption spectrum of IRC+10420 may be of help in this respect. In general, the strength of the DIBs correlates well with the interstellar reddening (e.g. Herbig 1995), but as early as in 1972, Snow & Wallerstein recognized that in the cases of mass-losing objects, where a fraction of the extinction may be provided by the circumstellar rather than interstellar dust, the reddening traced by the DIBs is significantly lower than the total *E(B–V)* would imply. The effect that DIBs trace less than the total reddening has also been seen towards other types of object, such as T Tauri stars (Meyer & Ulrich 1984), star forming regions (e.g. Adamson et al. 1991) and massive Young Stellar Objects (Oudmaijer et al. 1997). In all these cases there is, next to the diffuse ISM, an extra dust component, either circumstellar material, the molecular cloud material in which these objects are still embedded or a combination of both, responsible for the total extinction towards these objects. Although not yet well understood, this probably means that the physical conditions in the "DIB deficient" material are apparently such that the DIB carriers have failed to form, or are not excited in the same abundance and manner, as in the Interstellar Medium.

If one then considers the possibility that the DIB absorption does not, or hardly takes place in the circumstellar envelope of IRC+10420 , it may provide a rough value of the interstellar extinction towards the object. This is an important quantity for studies of the spectral energy distribution. In the event that a fraction of the DIB absorption does take place in its circumstellar envelope (see Le Bertre & Lequeux 1993 on such possibilities), we at least obtain a more stringent upper limit to the value of the interstellar reddening.

To this end, we searched the spectrum of IRC+10420 for DIBs listed in the catalog of JD94. Since the free spectral range of the individual spectral orders is relatively small, no broad DIBs were found. After carefully selecting the strongest, least affected lines by blends with stellar lines, we found 30 DIBs stronger than 20 mÅ. These are listed in Table 2. Four DIBs in the spectrum of IRC+10420 have also been measured by Le Bertre & Lequeux (1993). The measurements of the narrow $\lambda\lambda$ 5780, 5797 bands agree very well (Le Bertre & Lequeux

measured 580 and 270 mÅ respectively), the broad λ6177 measured by them is not visible in our higher resolution data. The EW of the λ6284 band (2200 Å), is blended with the much broader λ6281 line and is affected in the same way. We only measured the weaker λ6284 line.

In Table 2, the EW per unit *E(B–V)* as determined by JD94 and their respective ratio (which can be considered as the *E(B–V)* as traced by the DIBs) are listed. The scatter in the inferred DIB-*E(B–V)* is fairly large, the unweighted mean and standard deviation is 1.4 ± 0.5, yet it is clear that the reddening traced by the DIBs, as in the cases mentioned above, is smaller than the total reddening to IRC+10420 . Several DIBs appear to trace the total *E(B–V)*. It is not clear however whether this is due to an enhanced DIB formation efficiency in the circumstellar material, or whether it is due to the particular line of sight, as some lines of sight can show a remarkable deviations from the usual correlations between DIB strength and *E(B–V)* (Ehrenfreund et al. 1997). On the whole however, a larger sample of DIBs return approximately the same correlation value (Herbig 1995; JD94).

An additional clue to the origin of the DIBs may be provided with their central velocities. JD94 provide "rest" wavelengths of the DIBs with their associated errors. We have measured the Doppler shifts for the lines, which are listed in Table 2 in the last column. For some lines, especially the broader ones, it was not possible to measure the central velocities, and these entries are left blank. The average velocity, and its standard deviation is 18 ± 7 km s^{-1} (LSR). Some lines have markedly larger velocities, but the error in the central wavelength for these lines is large (see JD94). Indeed, when the 9 lines whose error in rest wavelength is less than 0.1 Å are selected, we obtain 17 ± 3 km s^{-1}. This is a blue-shift of ~ 60 km s^{-1} with respect to the systemic velocity, and even more than 80 km s^{-1} from most absorption lines. As the outflow velocity of the circumstellar material is only 40 km s^{-1} (Paper I), it seems likely that the DIBs indeed originate in the ISM in the line of sight instead of in the circumstellar material.

From this exercise, we find that the DIB strengths indicate a rough value of the interstellar *E(B–V)* towards IRC+10420 of 1.4 ± 0.5. The interstellar nature of the bands is supported by their Local Standard of Rest velocities, whose offset exceeds that of the stellar outflow velocity.

Table 2. Diffuse Interstellar Bands stronger than 20 mÅ and narrower than 3 Å. The first column denotes the wavelength of the DIB, the second the equivalent width (EW) of the features in the spectrum of IRC+10420. The errors in the measured EW is of order 20%. The third column represents the normalization EW to unit reddening as derived by JD94. The fourth column is the ratio of the latter two, finally the last column is the LSR velocity of the centre of the line, in the cases where it could be measured to 10 km s^{-1} certainty

λ (Å)	EW (mÅ)	EW/*E(B–V)* (mÅ)	ratio	$V_{\rm LSR}$ (km s^{-1})
4727.06	150	87	1.72	
4762.57	75	79	0.95	
4963.96	26	16	1.63	17
5766.25	30	13	2.31	5
5780.59	540	579	0.93	14
5797.11	240	132	1.82	15
5844.19	150	77	1.95	
5849.78	110	48	2.29	20
6004.55	25	24	1.04	
6089.80	45	17	2.65	18
6196.19	70	61	1.15	8
6203.19	150	107	1.40	14
6284.31	650	618	1.05	
6367.22	22	17	1.29	22
6376.07	40	26	1.54	17
6379.27	155	78	1.99	16
6449.13	45	20	2.25	24
6597.39	25	19	1.32	17
6613.72	260	231	1.13	13
6660.64	60	51	1.18	19
6699.37	40	41	0.98	12
6919.25	40	53	0.75	
6993.18	105	116	0.91	14
7060.81	40	19	2.11	32
7062.70	25	23	1.09	18
7334.33	30	60	0.50	24
7366.61	45	42	1.07	40
7562.24	70	87	0.80	16
8026.21	40	42	0.95	22
8037.24	30	37	0.81	20

4. Final remarks

In this paper we have presented the optical spectrum of the hypergiant IRC+10420 in July 1994. The high resolution spectrum was obtained using the Utrecht Echelle Spectrograph mounted on the 4.2 m WHT in La Palma. The total integration time was in excess of 9 hours, of which almost 7 hours was spent on the blue spectrum. A preliminary analysis of the spectrum yields the following conclusions:

1) The spectral type of IRC+10420 has changed from F8 in 1973 to A type in 1994. This implies that the temperature of IRC+10420 has increased by $1000 - 2000$ K. This is consistent with the picture that is nowadays sketched for the evolution of massive stars that have undergone a strong mass loss in the Red SuperGiant phase. The strong mass loss prevents the star from collapsing, allows the star to evolve back to the blue in the HR diagram, and speeds up the transition significantly. Evolutionary calculations presented by García-Segura et al. (1996) show that a 35 $M_\odot$ object that had a large mass loss on the

Red Supergiant Branch can evolve from the RSG to the Wolf-Rayet phase in a few hundred years.

2) The profiles and central velocities of all lines in IRC+10420 are very complex. Adopting the systemic velocity from the CO submillimetre rotational lines, it appears that many emission lines are blue-shifted with respect to the systemic velocity, while virtually all absorption lines are red-shifted. Clearly, these observations provide a challenge to understand the underlying astrophysical processes and the nature of the star. Taking the red-shifted absorption at face value, it is possible that IRC+10420 currently undergoes infall of material. A further analysis of the spectrum and a study of the related variability of the object is beyond the scope of this paper, and will be presented in a future paper (Oudmaijer et al., A&A in preparation).

3) The DIB absorption spectrum of IRC+10420 shows that the *E(B–V)* as traced by the DIBs is smaller than the total *E(B–V)* measured for the object. Assuming that the DIBs only trace the interstellar medium, as supported by kinematic information, and as found before in similar cases, we find that the interstellar extinction suffered by IRC+10420 is $E(B–V) = 1.4 \pm 0.5$.

Acknowledgements. We thank Reynier Peletier, Derek Jones and Ed Zuiderwijk for carrying out service observations of IRC+10420 . Roberta Humphreys is thanked for interesting discussions. The referee, Dr. T. Le Bertre is thanked for his useful comments. RDO received financial support under grant No. 782-372-031 from the Netherlands Foundation for Research in Astronomy (ASTRON) which receives its funds from the Netherlands Organisation for Scientific Research (NWO), and is now funded through a PDRA grant of the Particle Physics and Astronomy Research Council of the United Kingdom. The William Herschel Telescope and Isaac Newton Telescope are operated on the island of La Palma by the Royal Greenwich Observatory in the Spanish Observatorio del Roque de los Muchachos of the Instituto de Astrofísica de Canarias. Interested readers can obtain the spectroscopic data by contacting the author.

References

Adamson A.J., Whittet D.C.B., Duley W.W., 1991, MNRAS 252, 234
Ehrenfreund P., Cami J., Dartois E., Foing B.H., 1997, A&A 318, L28
Fix J.D., 1981, ApJ 248, 542
Fuhr J.R., Martin G.A., Wiese W.L., 1988, J. Phys. Chem. Ref. Data, Vol. 17, Suppl. 4 (Fe - Ni)
García-Segura G., Langer N., Mac Low M.-M., 1996, A&A 316, 133
Humphreys R.M., Strecker D.W., Murdock T.L., Low F.J., 1973, ApJ 179, L53
Humphreys R.M., 1991, in "Wolf-Rayet stars and interrelations with other massive stars in galaxies", van der Hucht K.A. and Hidayat K. (eds.), The Netherlands, p. 485
Herbig G.H., 1995, ARA&A 33, 19
Irvine C.E., 1986, IAU Circ. 4286
Jenniskens P., Désert F.-X., 1994, A&AS 106, 39 (JD94)
Jones T.J., et al., 1993, ApJ 411, 323
Kastner J.H., Weintraub D., 1995, ApJ 452, 833
Klochkova V.G., Chentsov E.L., Panchuk V.E., 1997, MNRAS 292, 19
Le Bertre T., Lequeux J., 1993, A&A 274, 909
Martin G.A., Fuhr J.R., Wiese W.L., 1988, J. Phys. Chem. Ref. Data, Vol. 17, Suppl. 3 (Sc - Mn)
Meyer D.M., Ulrich R.K., 1984, ApJ 283, 98
Moore C.E., 1945, "A multiplet table of astrophysical interest", Contribution from the Princeton University Observatory No. 20
Nedoluha G.E., Bowers P.F., 1992, ApJ 392, 249
Oudmaijer R.D., Bakker E.J., 1994, MNRAS 271, 615
Oudmaijer R.D., Busfield G., Drew J.E., 1997, MNRAS 291, 797
Oudmaijer R.D., Geballe T.R., Waters L.B.F.M., Sahu K.C., 1994, A&A 281, L33
Oudmaijer R.D., Groenewegen M.A.T., Matthews H.E.M., Blommaert J.A.D.L., Sahu K.C., 1996, MNRAS 280, 1062 (Paper I)
Snow T.P., Wallerstein G., 1972, PASP 84, 492
Tody D., 1993, in Astronomical Data Analysis Software and Systems II, Hanisch R.J., Brissenden R.J.V., Barnes J. (eds.) ASP Conf. Ser. 52, 173
Unger S., 1994, La Palma Technical Notes No. XXIII
Wiese W.L., Smith M.W., Glennon B.M., 1966, "Atomic Transition Probabilities, Vol. II Hydrogen through Neon", Nat. Stand. Ref. Data Ser. 20
Wiese W.L., Smith M.W., Miles B.M., 1969, "Atomic Transition Probabilities, Vol. II Sodium through Calcium", Nat. Stand. Ref. Data Ser. 22
Začs L.A., Klochkova V.G., Panchuk V.E., Spēlmanis R. 1996, MNRAS 282, 1171

A. The spectrum of IRC+10420

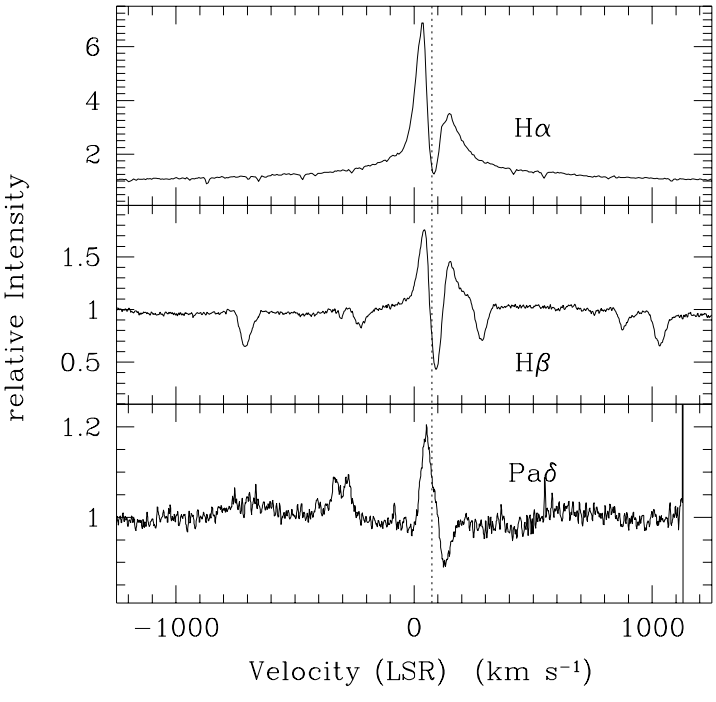

Fig. 3. The Hα, (from the INT spectrum), Hβ and Paδ lines in the spectrum. The horizontal line indicates the systemic velocity of 75 km s^{-1}

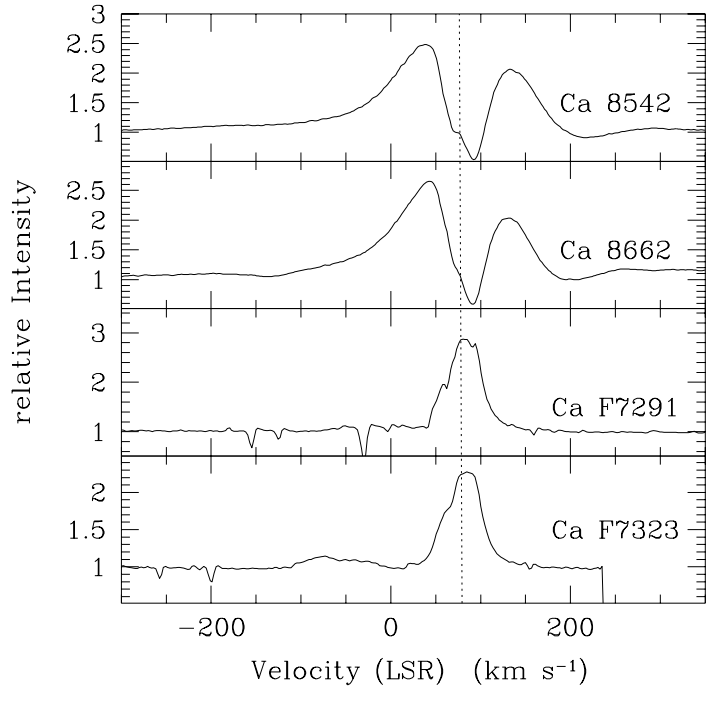

Fig. 4. The permitted and forbidden CaII lines. The λ8498 line of the CaII (2) triplet is similar to the other lines, and not shown. Due to the small free spectral range, and the subsequent uncertainties in the continuum rectifying of the spectrum, it is not clear whether the line-wings extend to the same velocities as Hα

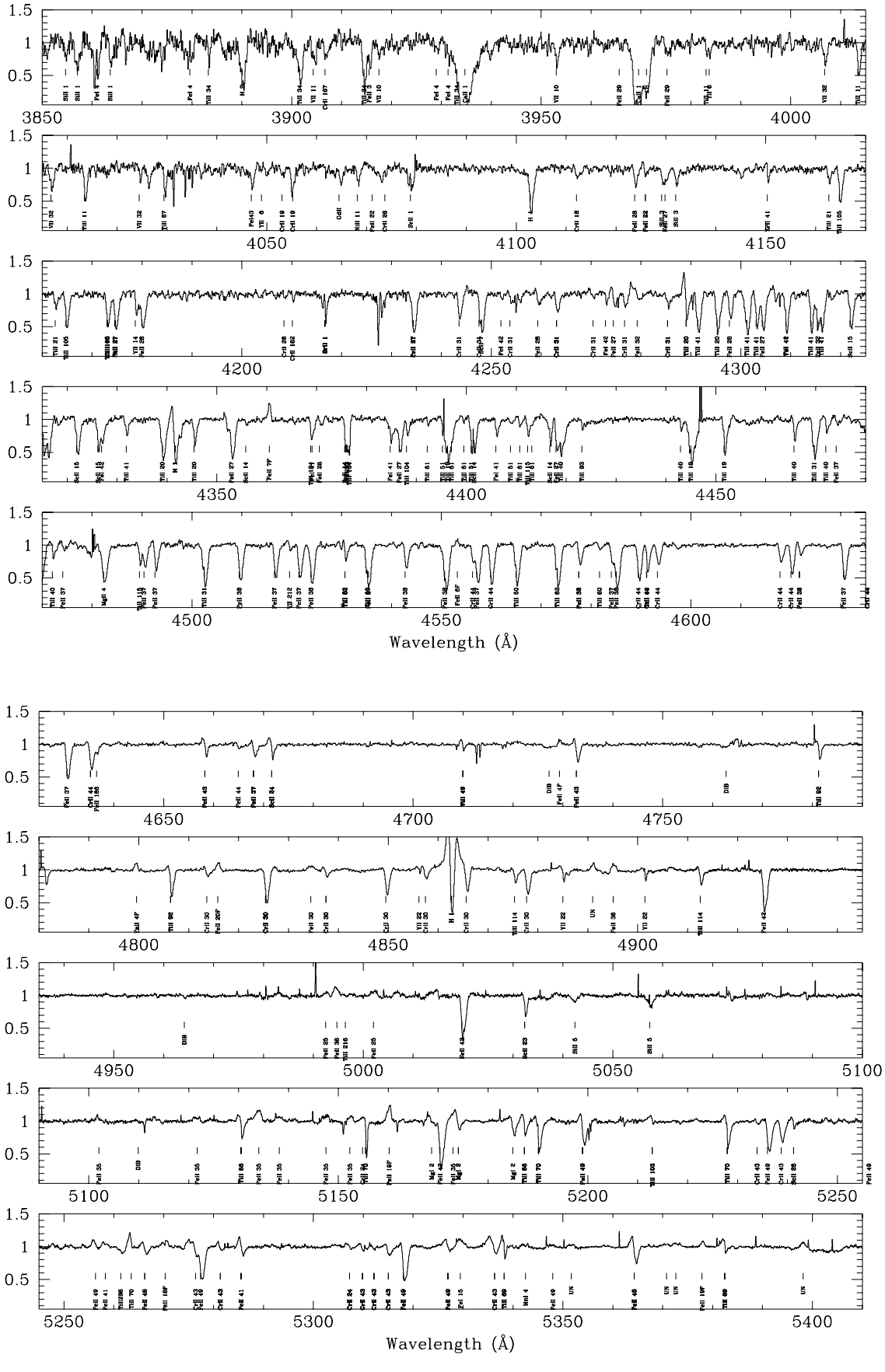

Fig. 5. The spectrum of IRC+10420 from 3850 Å to 1 μm. The lines are marked with their identifications. For clarity, the spectrum has been rebinned to pixels of 0.1 Å shortward of 4900 Å. The spikes in the spectrum are the result of the alignment of the individual orders. Very strong saturated telluric lines are not canceled out completely in the 7000 Å and 9000 Å regions

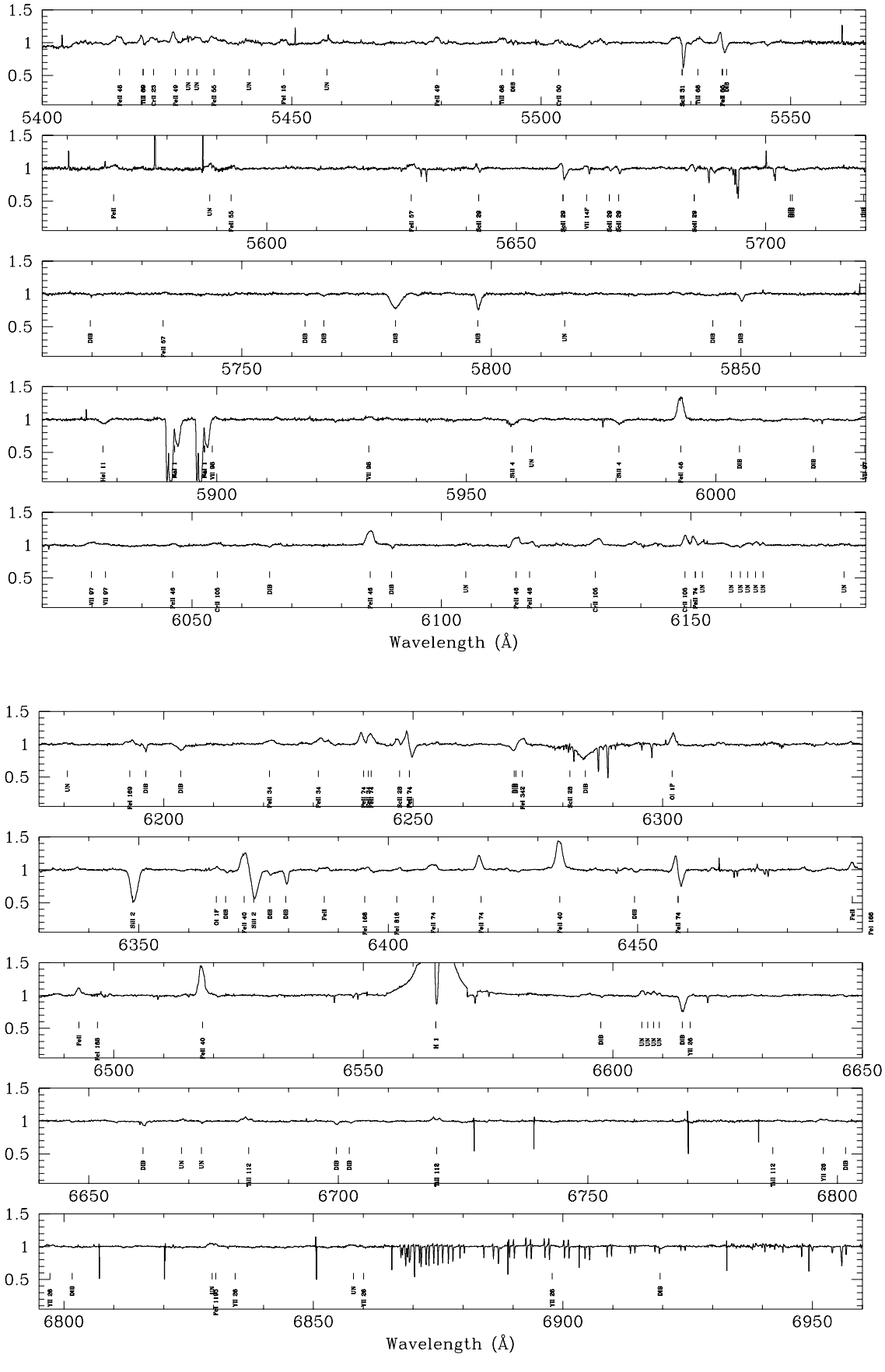

Fig. 5. continued

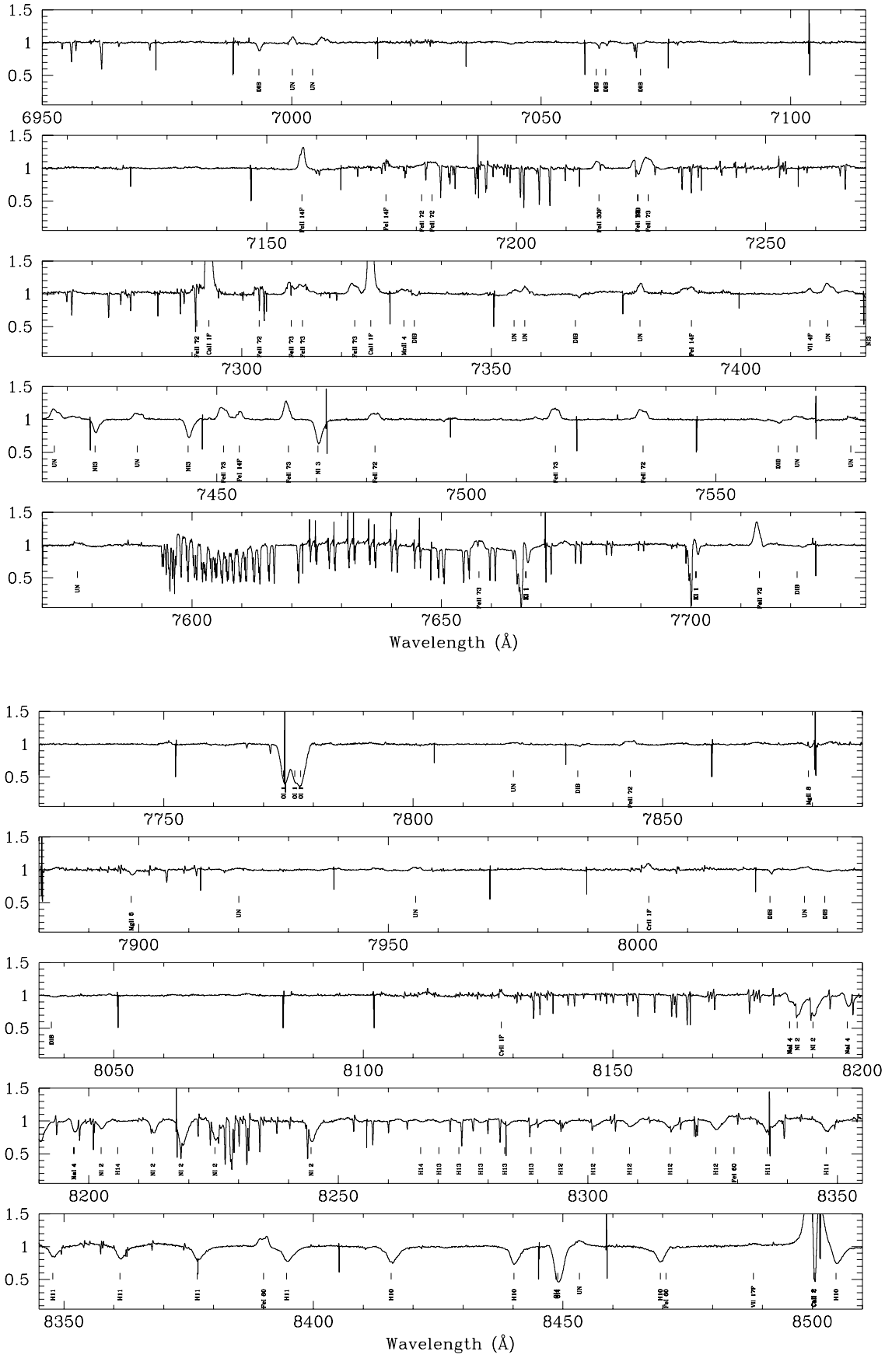

Fig. 5. continued

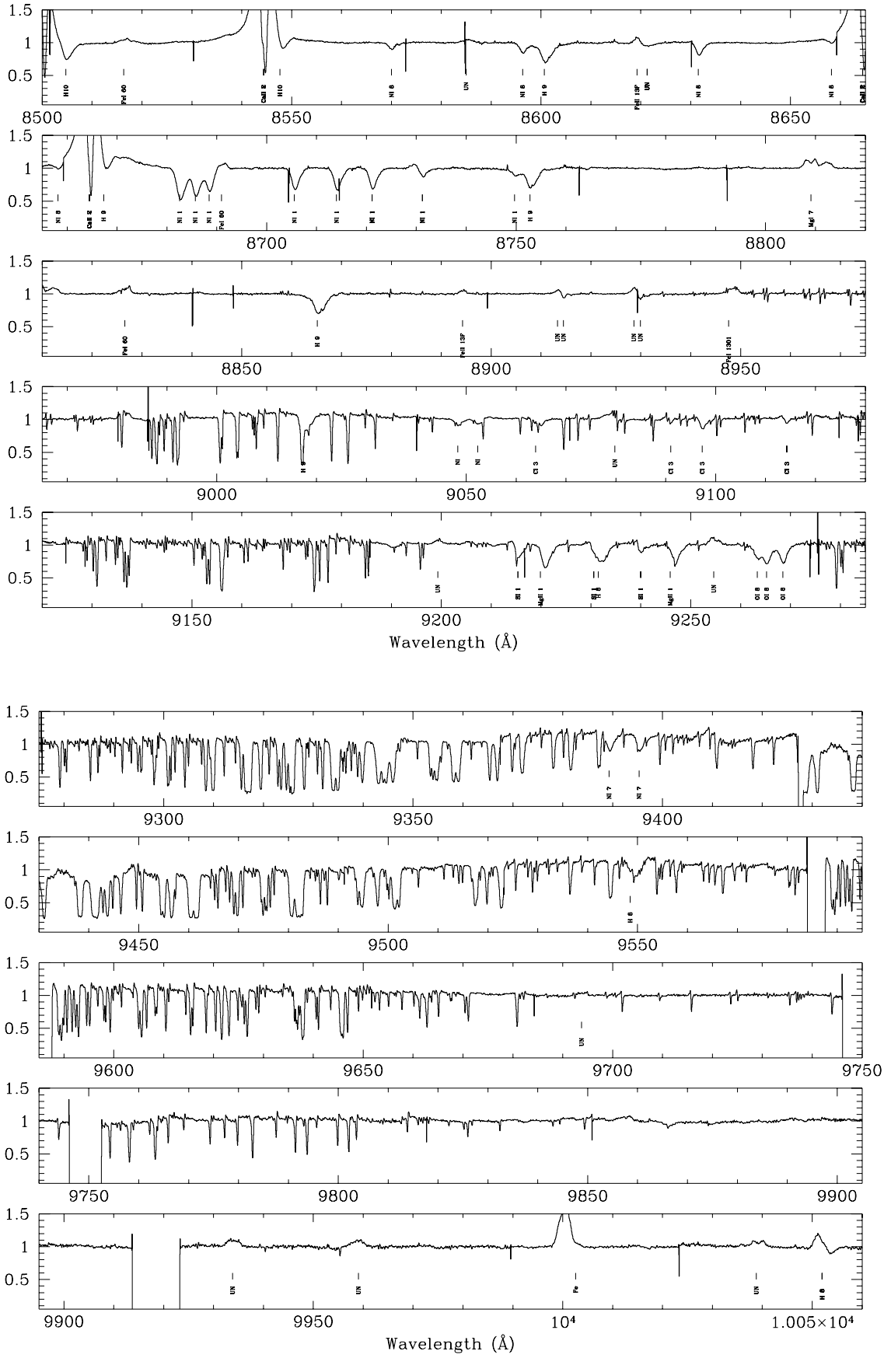

Fig. 5. continued